

Stable crystalline lattices in two-dimensional binary mixtures of dipolar particles

L. ASSOUD, R. MESSINA and H. LÖWEN

Institut für Theoretische Physik II: Weiche Materie, Heinrich-Heine-Universität Düsseldorf - Universitätsstrasse 1, D-40225 Düsseldorf, Germany

received 15 June 2007; accepted in final form 13 September 2007

published online 10 October 2007

PACS 82.70.Dd – Colloids

PACS 61.50.Ah – Theory of crystal structure, crystal symmetry; calculations and modeling

PACS 61.66.Dk – Alloys

Abstract – The phase diagram of binary mixtures of particles interacting via a pair potential of parallel dipoles is computed at zero temperature as a function of composition and the ratio of their magnetic susceptibilities. Using lattice sums, a rich variety of different stable crystalline structures is identified including $A_m B_n$ structures. (A (B) particles correspond to large (small) dipolar moments.) Their elementary cells consist of triangular, square, rectangular or rhombic lattices of the A particles with a basis comprising various structures of A and B particles. For small (dipolar) asymmetry there are intermediate AB_2 and A_2B crystals besides the pure A and B triangular crystals. These structures are detectable in experiments on granular and colloidal matter.

Copyright © EPLA, 2007

While the freezing transition and the corresponding crystal lattice in one-component systems is well understood by now [1,2], binary mixtures of two different particle species exhibits a much richer possibility of different solid phases. For example, while a one-component hard-sphere system freezes into the close-packed face-centered-cubic lattice [3], binary hard-sphere mixtures exhibit a huge variety of close-packed structures depending on their diameter ratio. These structures include AB_n superlattices, where A are the large and B the small spheres, with $n = 1, 2, 5, 6, 13$. These structures were found in theoretical calculations [4], computer simulations [5,6] and in real-space experiments on sterically stabilized colloidal suspensions [7,8]. Much less is known for soft repulsive interparticle interactions; most recent studies on crystallization include attractions and consider Lennard-Jones mixtures [9,10] or oppositely charged colloidal particles [11–13].

In this letter we explore the phase diagram of a binary mixture interacting via a soft repulsive pair potential proportional to the inverse cube of the particle separation. Using lattice sums, we obtain the zero-temperature phase diagram as a function of composition and asymmetry, *i.e.* the ratio of the corresponding prefactors in the particle-particle interaction. Our motivation to do so is threefold:

i) First there is an urgent need to understand the effect of softness in general and in particular in two spatial dimensions. The case of hard interactions in two spatial dimensions, namely binary hard disks, has been obtained by Likos and Henley [14] for a large range of diameter ratios. A complex phase behavior is encountered and it is unknown how the phase behavior is affected and controlled by soft interactions.

ii) The model of dipolar particles considered in this letter is realized in quite different fields of physics. Dipolar *colloidal particles* can be realized by imposing a magnetic field [15]. In particular, our model is realized by micron-sized superparamagnetic colloidal particles which are confined to a planar water-air interface and exposed to an external magnetic field parallel to the surface normal [15–19]. The magnetic field induces a magnetic dipole moment on the particles whose magnitude is governed by the magnetic susceptibility. Hence their interaction potential scales like that between two parallel dipoles with the inverse cube of the particle distance. Binary mixtures of colloidal particles with different susceptibilities have been studied for colloidal dynamics [20], fluid clustering [21,22], and the glass transition [23]. A complementary way to obtain dipolar colloidal particles is a fast alternating electric field which generates effective dipole moments in the colloidal

particles [24]. This set-up has been applied for two-dimensional binary mixtures in ref. [25]. In *granular matter*, the model has been realized by mixing millimeter-sized steel and brass spheres [26] which are placed on a horizontal plate and exposed to a vertical magnetic field such that the repulsive dipole-dipole interaction is the leading term. Stable triangular AB_2 crystalline lattices were found [26]. Layers of *dusty plasmas* involve particles whose interactions can be dominated by that of dipoles [27–29]. Other situations where two-dimensional mixtures of parallel dipoles are relevant concern *amphiphiles* (confined to a monomolecular film at an air-water interface [30]), *binary monolayers* [31–33], *ferrofluid* monolayers [34] exposed to a perpendicular magnetic field, or thin films of *molecular* mixtures (*e.g.* of boron nitride and hydrocarbon molecules) with a large permanent dipole moment [35]. Hence, in principle, our results can be directly compared to various experiments of (classical) dipolar particles with quite different size in quite different set-ups.

iii) It is important to understand the different crystalline sub-structures in detail, since a control of the colloidal composite lattices may lead to new optical band-gap materials (so-called photonic crystals) [36] to molecular-sieves [37] and to micro- and nano-filters with desired porosity [38]. Nano-sieves and filters can be constructed on a colloidal monolayer confined at interfaces [38]. Their porosity is directly coupled to their crystalline structure. For these applications, it is mandatory to understand the different stable lattice types which occur in binary mixtures.

As a result, we find a variety of different stable composite lattices. They include $A_m B_n$ structures with, for instance, $n = 1, 2, 4, 6$ for $m = 1$. Their elementary cells consist of (equilateral) triangular, square, rectangular and rhombic lattices of the A particles. These are highly decorated by a basis involving either B particles alone or both B and A particles. The topology of the resulting phase diagram differs qualitatively from that of hard-disk mixtures [14]. For small (dipolar) asymmetries, for instance, we find intermediate AB_2 and $A_2 B$ structures besides the pure triangular A and B lattices which are absent for hard disks. Our calculations admit more candidate phases than considered in earlier investigations [39] where two-dimensional quasicrystals were shown to be metastable. We further comment that we expect that colloidal glasses in binary mixtures of magnetic colloids [23] are metastable as well but need an enormous time to phase separate into their stable crystalline counterparts.

The model systems used in our study are binary mixtures of dipolar particles made up of two species denoted as A and B . Each component A and B is characterized by its dipole moment \mathbf{m}_A and \mathbf{m}_B , respectively. The particles are confined to a two-dimensional plane and the dipole moments are fixed in the direction perpendicular to the plane. Thereby the dipole-dipole interaction

is repulsive. Introducing the ratio $m = m_B/m_A$ of dipole strengths m_A and m_B , the pair interaction potentials between two A dipoles, a A - and B -dipole, and two B -dipoles at distance r are

$$\begin{aligned} V_{AA}(r) &= V_0 \varphi(r), & V_{AB}(r) &= V_0 m \varphi(r), \\ V_{BB}(r) &= V_0 m^2 \varphi(r), \end{aligned} \quad (1)$$

respectively. The dimensionless function $\varphi(r)$ is equal ℓ^3/r^3 , where ℓ stands for a unit length. The amplitude V_0 sets the energy scale.

Our task is to find the stable crystalline structures adopted by the system at zero temperature. We consider a parallelogram as a primitive cell which contains n_A A -particles and n_B B -particles. This cell can be described geometrically by the two lattice vectors $\mathbf{a} = a(1, 0)$ and $\mathbf{b} = a\gamma(\cos\theta, \sin\theta)$, where θ is the angle between \mathbf{a} and \mathbf{b} and γ is the aspect ratio ($\gamma = |\mathbf{b}|/|\mathbf{a}|$). The position of a particle i (of species A) and that of a particle j (of species B) in the parallelogram is specified by the vectors $\mathbf{r}_i^A = (x_i^A, y_i^A)$ and $\mathbf{r}_j^B = (x_j^B, y_j^B)$, respectively. The total internal energy (per primitive cell) U has the form

$$\begin{aligned} U &= \frac{1}{2} \sum_{J=A,B} \sum_{i,j=1}^{n_J} \sum_{\mathbf{R}}' V_{JJ} (|\mathbf{r}_i^J - \mathbf{r}_j^J + \mathbf{R}|) \\ &+ \sum_{i=1}^{n_A} \sum_{j=1}^{n_B} \sum_{\mathbf{R}} V_{AB} (|\mathbf{r}_i^A - \mathbf{r}_j^B + \mathbf{R}|), \end{aligned} \quad (2)$$

where $\mathbf{R} = k\mathbf{a} + l\mathbf{b}$ with k and l being integers. The sums over \mathbf{R} in eq. (2) run over all lattice cells where the prime indicates that for $\mathbf{R} = \mathbf{0}$ the terms with $i = j$ are to be omitted. In order to handle efficiently the long-range nature of the dipole-dipole interaction, we employed a Lekner-summation [40,41].

We choose to work at prescribed pressure p and zero temperature ($T = 0$). Hence, the corresponding thermodynamic potential is the Gibbs free energy G . Additionally, we consider interacting dipoles at composition $X := n_B/(n_A + n_B)$, so that the (intensive) Gibbs free energy g per particle reads: $g = g(p, m, X) = G/(n_A + n_B)$. At $T = 0$, g is related to the internal energy per particle $u = U/(n_A + n_B)$ through $g = u + p/\rho$, where the pressure p is given by $p = \rho^2(\partial u/\partial \rho)$, and $\rho = (n_A + n_B)/|\mathbf{a} \times \mathbf{b}|$ is the total particle density. The Gibbs free energy per particle g has been minimized with respect to γ , θ and the position of particles of species A and B within the primitive cell. To reduce the complexity of the energy landscape, we have limited the number of variables and considered the following candidates for our binary mixtures: $A_4 B$, $A_3 B$, $A_2 B$, $A_4 B_2$, $A_3 B_2$, AB , $A_2 B_2$, $A_2 B_3$, AB_2 , $A_2 B_4$, AB_3 , AB_4 and AB_6 . For the AB_6 case we considered a triangular lattice formed by the A particles.

The final phase diagram in the (m, X) -plane has been obtained by using the common tangent construction. The dipole-strength ratio m can vary between zero and unity. A low value of m (*i.e.*, close to zero) corresponds to a large

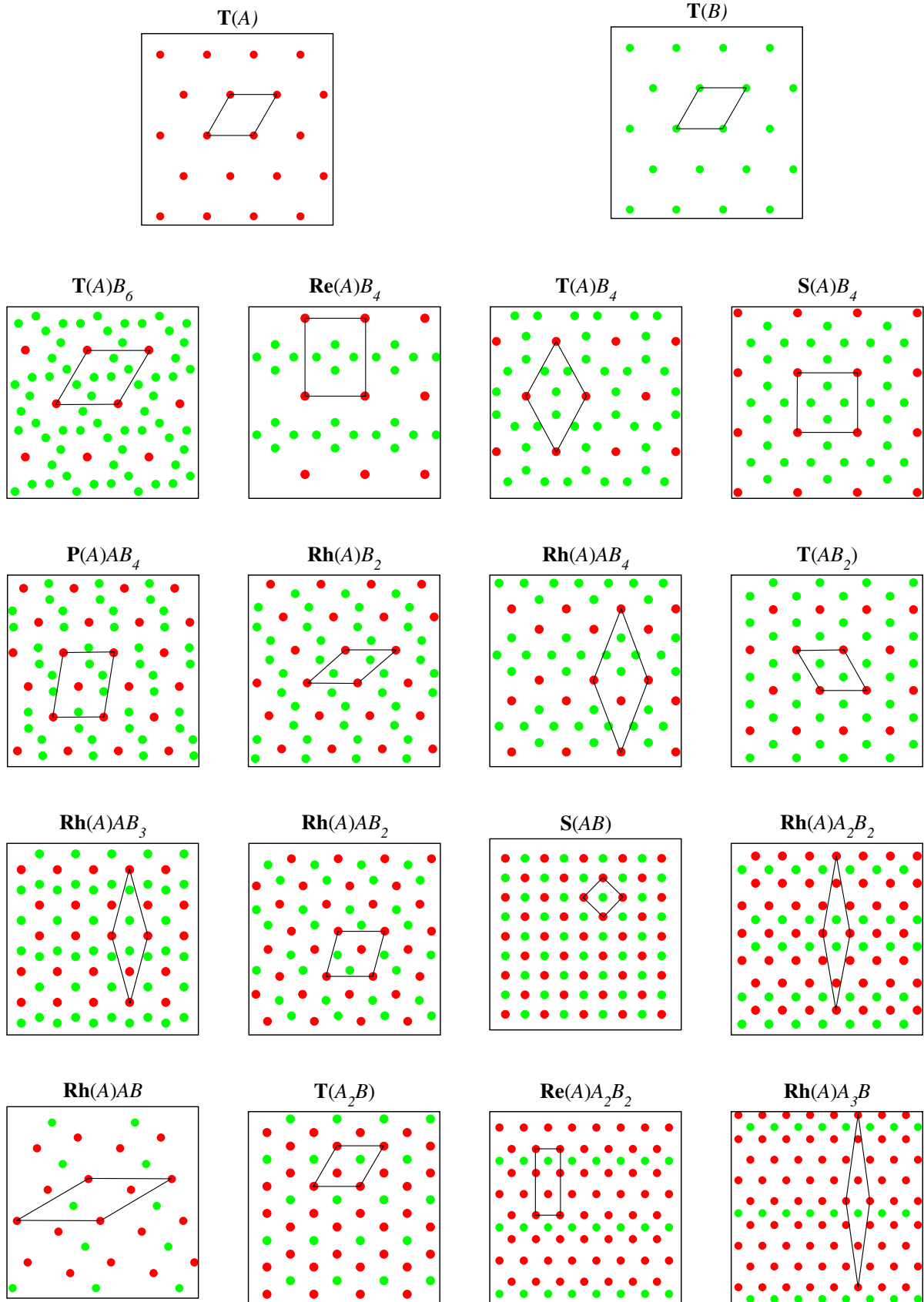


Fig. 1: (Colour on-line) The stable binary crystal structures and their primitive cells. The red/dark (green/light) discs correspond to A (B) particles.

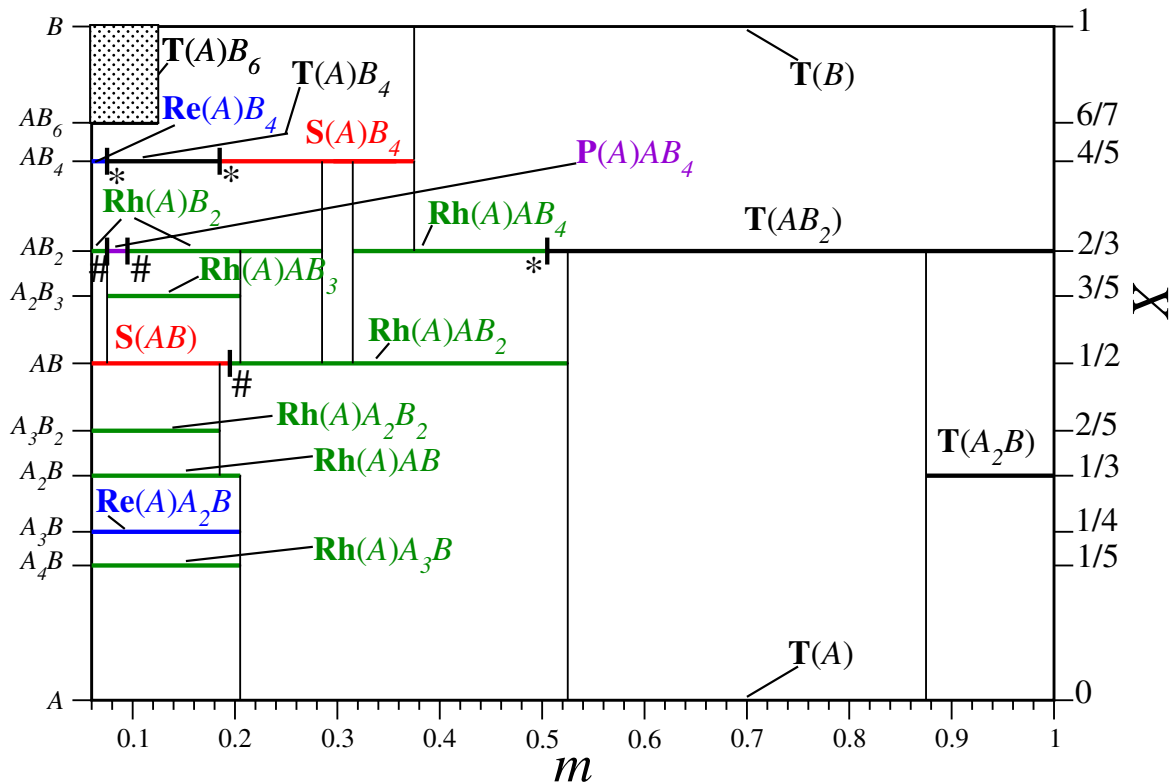


Fig. 2: (Colour on-line) The phase diagram in the (m, X) -plane of dipolar asymmetry and composition at $T = 0$. The gray box denotes an unknown region. The symbol # (*) denote continuous (discontinuous) transitions.

Table 1: The stable phases with their Bravais lattice and their basis.

Phase	Bravais lattice [basis]
$\mathbf{T}(A)$	Triangular for A [one A particle]
$\mathbf{T}(B)$	Triangular for B [one B particle]
$\mathbf{S}(AB)$	Square for A and B together [one A and one B particles]
$\mathbf{S}(A)B_n$	Square for A [one A and n B particles]
$\mathbf{Re}(A)A_mB_n$	Rectangular for A [$(m+1)$ A and n B particles]
$\mathbf{Rh}(A)A_mB_n$	Rhombic for A [$(m+1)$ A and n B particles]
$\mathbf{P}(A)AB_4$	Parallelogram for A [two A and four B particles]
$\mathbf{T}(AB_2)$	Triangular for A and B together [one A and two B particles]
$\mathbf{T}(A_2B)$	Triangular for A and B together [two A and one B particles]
$\mathbf{T}(A)B_n$	Triangular for A [one A and n B particles]

dipole-strength asymmetry, whereas a high one (*i.e.*, close to unity) indicates a weak dipole-strength asymmetry. Our calculations show that all the mixtures, except AB_3 and A_4B_2 , are stable. Their corresponding crystalline

lattices are depicted in fig. 1 and the nomenclature is explained in table 1. For the one component case ($X = 0$ (pure A) and $X = 1$ (pure B), see fig. 2), we found an equilateral triangular lattice $\mathbf{T}(A)$ and $\mathbf{T}(B)$, respectively, as expected (see fig. 1).

The most relevant and striking findings certainly concern the phase behavior at weak dipole-strength asymmetry ($0.5 \lesssim m < 1$), see fig. 2. Thereby, the only stable mixture AB_2 over such a large range of m corresponds to the (“globally” triangular) phase $\mathbf{T}(AB_2)$ (see fig. 1 and fig. 2). This is in strong contrast to what occurs with hard-disk potentials [14], where *no* mixture sets in at low size asymmetry. At sufficiently low dipole-strength asymmetry ($m > 0.88$), see fig. 2, the mixture A_2B , that also corresponds to a globally triangular crystalline structure (namely $\mathbf{T}(A_2B)$, see fig. 1), is equally stable. The stability in the limit $m \rightarrow 1$ of those globally triangular structures are fully consistent with the fact that one-component dipolar systems are triangular.

In the regime of strong dipole-strength asymmetry ($0.06 < m \lesssim 0.5$), see fig. 2, the stability of the composition $X = 1/2$, corresponding to the mixtures AB and A_2B_2 , is dominant and the phase diagram gets richer involving all the different structures (except $\mathbf{T}(AB_2)$) shown in fig. 1. More specifically, for the composition $X = 1/2$, we have two phases $\mathbf{S}(AB)$ and $\mathbf{Rh}(A)AB_2$. The transition between these two phases is continuous as marked by a symbol # in fig. 2. For $X = 2/3$, many stable phases

emerge as depicted in fig. 2. In the B -rich region at large asymmetry, the stability will involve many different structures which are probably not considered here. Therefore we leave this region open, see the gray box in fig. 2. Below $X = 2/3$, at large asymmetry ($m \lesssim 0.2$), the true phase diagram will also involve a very dense spectrum of stable compositions, as suggested by the already many stable compositions (see fig. 2), which are not among the candidate structures considered here. This feature is very similar to the behavior reported in hard disk mixtures [14], where a *continuous* spectrum of stable mixtures is found for $X \leq 2/3$ at high size asymmetry. In the limit $m \rightarrow 0$, a triangular lattice for the A particles will be stable with an increasingly complex substructure of B particles.

In conclusion, the ground-state phase diagram of a monolayer of two-dimensional dipolar particles shows a variety of different stable solid lattices. The topology of the phase diagram is different from that of hard disks. Whereas short-ranged interactions lead to a phase separation into pure A and B crystals at low asymmetries, there are two intermediate A_2B and AB_2 mixtures for softer interactions. This explains the experimental findings of Hay and coworkers [26] who found an AB_2 crystal structure in millimeter-sized steel and brass spheres [26] which does not occur to be stable for hard particles. A further more quantitative experimental confirmation of our theoretical predictions are conceivable either in suspension of magnetic colloids or for binary charged colloidal suspensions [42] confined between two parallel glass plates [43] or for any other situation where two-dimensional dipolar particles are involved.

We finish with a couple of remarks: First, based on the present studies it would be interesting to study the behavior of tilted dipoles where anisotropies and attraction play a significant role [44]. Our data may also serve as a benchmark to perform further studies on melting of the composite crystals and crystal nucleation out of the melt in two spatial dimensions. The extension to one-component bilayers [45,46] made up of dipolar particles would certainly be relevant. It would also be interesting to apply the method of evolutionary algorithms [47] to the present problem in order to increase the basket of candidate phases.

We thank C. LIKOS, H. J. SCHÖPE and T. PALBERG for helpful discussions. This work has been supported by the DFG within the SFB-TR6, Project Section D1.

REFERENCES

- [1] HANSEN J. P., LEVESQUE D. and ZINN-JUSTIN J., *Liquids, Freezing and Glass Transition* (North-Holland, Amsterdam) 1992.
- [2] GROH B. and DIETRICH S., *Phys. Rev. E*, **63** (2001) 021203.
- [3] PRONK S. and FRENKEL D., *Phys. Rev. Lett.*, **90** (2003) 255501.
- [4] XU H. and BAUS M., *J. Phys.: Condens. Matter*, **4** (1992) L663.
- [5] ELDRIDGE M. D., MADDEN P. A. and FRENKEL D., *Nature*, **365** (1993) 35.
- [6] ELDRIDGE M. D., MADDEN P. A. and FRENKEL D., *Mol. Phys.*, **80** (1993) 987.
- [7] BARTLETT P., OTTEWILL R. H. and PUSEY P. N., *Phys. Rev. Lett.*, **68** (1992) 3801.
- [8] ELDRIDGE M. D., MADDEN P. A., PUSEY P. N. and BARTLETT P., *Mol. Phys.*, **84** (1995) 395.
- [9] VLOT M. J., HUITEMA H. E. A., DE VOOYS A. and VAN DER EERDEN J. P., *J. Chem. Phys.*, **107** (1997) 4345.
- [10] FERNANDEZ J. R. and HARROWELL P., *Phys. Rev. E*, **67** (2003) 011403.
- [11] HYNINEN A. P., LEUNISSEN M. E., VAN BLAADEREN A. and DIJKSTRA M., *Phys. Rev. Lett.*, **96** (2006) 018303.
- [12] HYNINEN A. P., CHRISTOVA C. G., VAN ROIJ R., VAN BLAADEREN A. and DIJKSTRA M., *Phys. Rev. Lett.*, **96** (2006) 138308.
- [13] LEUNISSEN M. E., CHRISTOVA C. G., HYNINEN A. P., ROYALL C. P., CAMPBELL A. I., IMHOF A., DIJKSTRA M., VAN ROIJ R. and VAN BLAADEREN A., *Nature*, **437** (2005) 235.
- [14] LIKOS C. N. and HENLEY C. L., *Philos. Mag. B*, **68** (1993) 85.
- [15] ZAHN K., MENDEZÁLCARAZ J. M. and MARET G., *Phys. Rev. Lett.*, **79** (1997) 175.
- [16] ZAHN K., LENKE R. and MARET G., *Phys. Rev. Lett.*, **82** (1999) 2721.
- [17] ZAHN K. and MARET G., *Phys. Rev. Lett.*, **85** (2000) 3656.
- [18] KÖPPL M., HENSELER P., ERBE A., NIELABA P. and LEIDERER P., *Phys. Rev. Lett.*, **97** (2007) 208302.
- [19] MANGOLD K., BIRK J., LEIDERER P. and BECHINGER C., *Phys. Chem. Chem. Phys.*, **6** (2004) 1623.
- [20] KOLLMANN M., HUND R., RINN B., NAGELE G., ZAHN K., KÖNIG H., MARET G., KLEIN R. and DHONT J. K. G., *Europhys. Lett.*, **58** (2002) 919.
- [21] HOFFMANN N., EBERT F., LIKOS C. N., LÖWEN H. and MARET G., *Phys. Rev. Lett.*, **97** (2006) 078301.
- [22] HOFFMANN N., LIKOS C. N. and LÖWEN H., *J. Phys.: Condens. Matter*, **18** (2006) 10193.
- [23] KÖNIG H., HUND R., ZAHN K. and MARET G., *Eur. Phys. J. E*, **18** (2005) 287.
- [24] YETHIRAJ A. and VAN BLAADEREN A., *Nature*, **421** (2003) 513.
- [25] KUSNER R. E., MANN J. A., KERINS J. and DAHM A. J., *Phys. Rev. Lett.*, **73** (1994) 3113.
- [26] HAY M. B., WORKMAN R. K. and MANNE S., *Phys. Rev. E*, **67** (2003) 012401.
- [27] RESENDES D. P., *Phys. Rev. E*, **61** (2000) 793.
- [28] KOURAKIS I. and SHUKLA P. K., *Phys. Plasmas*, **11** (2004) 3665.
- [29] FELDMANN J. D., KALMAN G. J. and ROSENBERG M., *J. Phys. A: Math. Gen.*, **39** (2006) 4549.
- [30] SEUL M., *Europhys. Lett.*, **28** (1994) 557.
- [31] HU Y. F., MELESON K. and ISRAELACHVILI J., *Biophys. J.*, **91** (2006) 444.
- [32] KELLER S. L. and MCCONNELL H. M., *Phys. Rev. Lett.*, **82** (1999) 1602.

- [33] MESSE L., PERDIGON A., CLARKE S. M., INABA A. and ARNOLD T., *Langmuir*, **21** (2005) 5085.
- [34] ELIAS F., FLAMENT C., BACRI J. C. and NEVEU S., *J. Phys. I*, **7** (1997) 711.
- [35] WIECHERT H. and KROMKER B., *J. Non-Cryst. Solids*, **307** (2002) 538.
- [36] MANOHARAN V. N., ELSESSER T. and PINE D. J., *Science*, **301** (2003) 483.
- [37] KECHT J., MIHALOVA B., KARAGHISOFF K., MINTOVA S. and BEIN T., *Langmuir*, **20** (2004) 5271.
- [38] YAN F. and GOEDEL W. A., *Chem. Mater.*, **16** (2004) 1622; *Nano Lett.*, **4** (2004) 1193.
- [39] SCHEFFLER F., MAASS P., ROTH J. and STARK H., *Europhys. J. B*, **42** (2004) 85.
- [40] LEKNER J., *Physica A*, **157** (1989) 826.
- [41] GRZYBOWSKI A. and BRODKA A., *Mol. Phys.*, **101** (2003) 1079.
- [42] WETTE P., SCHÖPE H. J. and PALBERG T., *J. Chem. Phys.*, **122** (2005) 144901.
- [43] FONTECHA A. B., SCHÖPE H. J., KÖNIG H., PALBERG T., MESSINA R. and LÖWEN H., *J. Phys.: Condens. Matter*, **17** (2005) S2779.
- [44] FROLTSOV V., BLAAK R., LIKOS C. N. and LÖWEN H., *Phys. Rev. E*, **68** (2003) 061406.
- [45] GOLDONI G. and PEETERS F. M., *Phys. Rev. B*, **53** (1996) 4591.
- [46] MESSINA R. and LÖWEN H., *Phys. Rev. Lett.*, **91** (2003) 146101.
- [47] GOTTWALD D., KAHL G. and LIKOS C. N., *J. Chem. Phys.*, **122** (2005) 204503.